Enhancement of magnetization damping coefficient of permalloy thin films with dilute Nd dopants

C. Luo,[1] Z. Feng,[2] Y. Fu,[1,3] W. Zhang,[1] P. K. J. Wong,[4] Z. X. Kou,[1] Y. Zhai,[1,2,*] H. F. Ding,[2] M. Farle,[3] J. Du,[2] and H. R. Zhai[2]

[1]*Physics Department, Southeast University, Nanjing 211189, China*

[2]*National Laboratory of Solid State Microstructures, Nanjing University, Nanjing 210093, China*

[3]*Fakultät für Physik and Center for Nanointegration Duisburg-Essen (CeNIDE), Universität Duisburg-Essen, 47048 Duisburg, Germany*

[4]*NanoElectronics Group, MESA+ Institute of Nanotechnology, University of Twente, P.O. Box 217, 7500 AE Enschede, Netherlands*

(Received 31 October 2013; revised manuscript received 5 May 2014; published 20 May 2014)

For spintronics application, which requires fast field switching, it is important to have a kind of soft magnetic material with large damping coefficient. Here, we present the studies of the Nd dopant-level-dependent damping coefficient of Nd_x-$Py_{(1-x)}$ thin films (30 nm) in a dilute region utilizing ferromagnetic resonance (FMR). With the Nd content increasing, the film structure was found to be changing from polycrystalline to amorphous when the Nd content is around 3.4%. Meanwhile, the magnetization decreases linearly. Interestingly, we find that along the easy axis, both low coercivity and high hysteresis squareness are simultaneously maintained in the system; i.e., the magnetic softness has been well kept. By theoretical fitting of the angular dependence of the FMR field, the first- and second-order magnetic anisotropy constants, K_1 and K_2, and the Lande g factor are obtained and discussed quantitatively. The measurements of angular and frequency dependence of the ferromagnetic resonance linewidth, as well as the theoretical fitting by considering the contributions of Gilbert damping, two-magnon scattering, and inhomogeneous broadening, show that the damping coefficient α increases rapidly (about 25-fold) as the Nd content increases to 11.6%, which is mainly due to the enhanced spin-orbit coupling by the Nd additives, supported by x-ray magnetic circular dichroism measurements.

DOI: 10.1103/PhysRevB.89.184412 PACS number(s): 75.50.Bb, 75.78.−n, 76.30.Kg, 76.50.+g

I. INTRODUCTION

The investigation of the magnetization damping behavior of thin films has attracted great interest due to their application in spintronics devices such as magnetic sensors, magnetic reading heads, and magnetic random access memory [1,2]. A new type of spin-torque nano-oscillator (STNO), composed of two perpendicular polarizers and two in-plane free layers, was proposed very recently [3]. This kind of dual free-layer STNO is believed to have the capability of generating large microwave power at frequencies greater than those attainable in STNOs with a single perpendicular polarizer. To improve the overall performance of such a STNO, the selection of materials with appropriate magnetization and its dynamic damping for the in-plane free layers is critical. On the one hand, increasing the damping is one method of broadening the frequency range of the oscillator operation; on the other hand, using magnetic materials with small saturation magnetization is beneficial for suppressing the critical current density. Thus, the permalloy (Py) thin films with rare-earth (RE) doping are good candidates, where the damping is enhanced and the magnetization is kept in the film plane and decreased with increasing RE.

Py is regarded as one of the most favored magnetic materials for spintronics application due to its excellent soft magnetic properties, such as appropriate magnetization and low coercivity. However, as the orbital moment is largely quenched in such a 3*d* transition-metal alloy, the damping of the magnetization is too low, which limits its application for magnetic devices requiring fast switching. It is known that the magnetization switching is the decaying magnetization procession motion process that occurs if a nonzero damping acts on the procession motion; the magnetization damping of the material is inversely proportional to the relaxation time (switching time) constant [4]. If the magnetization damping is too small, the switching time becomes very large, because the magnetization performs too many precession rotations before it finally points to the direction of the effective field, which is also confirmed by some experiments [5,6]. RE elements possess a large orbital moment, which could enhance the dynamic damping of RE-doped Py [7–12]. On the other hand, RE dopants might increase the magnetic anisotropy and make the soft magnetic films harder and thus require larger magnetic fields for reversing the magnetization [13–16]. For spintronics application, it is important to find the right dopants—those which not only enhance the dynamic damping but also maintain the soft magnetic properties of Py.

In early years, transition-metal (TM) films with RE doping have been extensively studied. Bailey *et al.* [7] compared the influence of Tb and Gd dopants on magnetization dynamics in Py thin films. Russek *et al.* [8] conducted a study on the magnetostriction and the damping of Tb-Py films. Woltersdorf *et al.* [10] presented experimental results on the magnetization dynamics of Py thin films doped with Ho, Tb, Gd, and Dy. Most of these studies focused on heavy RE impurities due to their large L-S coupling. The doping effects with light RE elements, however, have not been addressed as much. In theory, the magnetic moment of heavy RE atoms is antiparallel to the magnetic moment of Py atoms [17,18]. As a result, the magnetization decreases with increasing doping of heavy REs. In contrast, the magnetic moment between TMs and REs is parallel for the light RE dopants [19]. It would be interesting to explore how the magnetization damping and magnetic properties would change by introducing light RE impurities.

Ferromagnetic resonance (FMR) is one of the most powerful experimental techniques for studying magnetic properties of thin films and can provide sufficient information describing

*Corresponding author: yazhai@seu.edu.cn

the magnetic properties of thin films, such as magnetic moment, magnetic anisotropy, the Lande g factor, and relaxation mechanisms of the magnetization [20,21].

In this paper, we study the influence of Nd doping (0–11.6 at. %) on the magnetic properties of 30-nm-thick Py thin films. At 3.4% the structure of our films changes from polycrystalline to amorphous. The Gilbert damping coefficient at 11.6% Nd doping is found to be about 25 times larger than the value without doping, which might originate from the enhancement of L-S coupling. In addition, the various contributions of FMR linewidth are successfully separated. The inhomogeneous broadening and two-magnon scattering contributions for FMR linewidth in the Py films with different Nd dopant are analyzed. At the same time, the effective magnetization as well as the first- and second-order magnetic anisotropy constants K_1 and K_2, Lande g factor, etc., are determined by fitting the FMR experimental data.

II. EXPERIMENTAL METHOD

The Nd_x-$Py_{(1-x)}$ thin films (30 nm) were deposited on silicon substrates by dc magnetron sputtering with a base pressure of 1.2×10^{-5} Pa at room temperature. A 5-nm-thick Ta seed layer was first deposited onto the silicon surface. The Nd_x-$Py_{(1-x)}$ films were capped with a 5-nm-thick Ta layer to prevent oxidation. During deposition an Ar pressure of 0.5 Pa was kept, and a dc power of 30 W was used. A magnetic field of 5 mT was applied to induce a small in-plane uniaxial anisotropy. Nd was doped into the films by co-sputtering from a $Ni_{80}Fe_{20}$ alloy target with Nd chips located symmetrically in a ring on the target surface. The dopant concentration was adjusted by varying the number of Nd chips.

The composition of the films was determined by energy-dispersive x-ray fluorescence spectroscopy, and the structure of the films was investigated by x-ray diffraction (XRD). The static magnetic properties were measured by vibrating sample magnetometry (VSM). The ex situ ferromagnetic resonance was measured by a homemade vector network analyzer ferromagnetic resonance (VNA-FMR) [22] and electron spin resonance with a conventional transverse electric (TE) mode rectangular microwave resonance cavity in a scanning dc magnetic field (0–1400 mT) with a fixed frequency of 9.78 GHz.

III. RESULTS AND DISCUSSION

A. Structure and static magnetic properties

The atomic concentrations of Nd of the different films are 0, 1.7%, 3.4%, 5.1%, 7.3%, and 11.6%, respectively. As shown in Fig. 1, the XRD pattern of the films shows a clear crystalline diffraction peak of NiFe (111) texture for the undoped $Ni_{80}Fe_{20}$ film. The intensity of the NiFe (111) peak decreases with increasing Nd content and almost disappears in the noise background when the Nd content is around 3.4%, which indicates that the film crystalline structure has changed from polycrystalline to amorphous.

In-plane magnetic hysteresis loops are measured by applying the magnetic field perpendicular and parallel to the direction of induced uniaxial anisotropy in the film plane. The results are partly shown in the inset of Fig. 2. The remanent magnetization of the in-plane hysteresis loops along

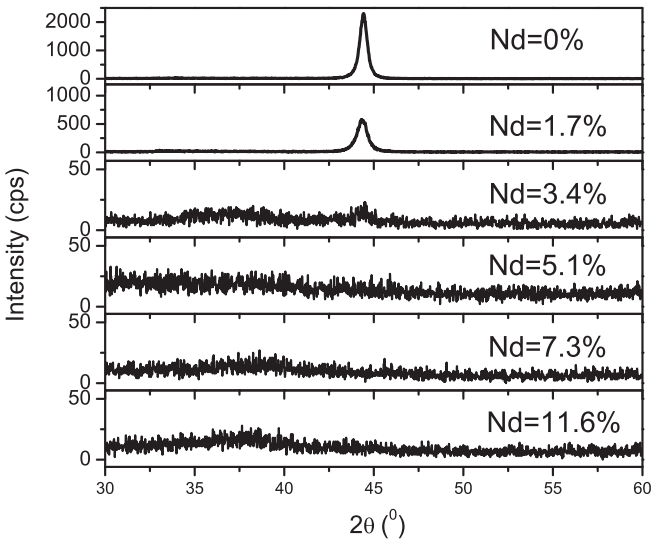

FIG. 1. XRD patterns for Nd_x-$Py_{(1-x)}$ thin films.

the easy axis is kept high with increasing content of Nd from 0% to 11.6%. The anisotropy between in-plane hysteresis loops along the easy and hard axes increases. Quantitatively, the coercivity H_c increases with increasing Nd content but remains small. H_c has a maximum value of 0.62 mT when Nd content is 5.1%, indicating that Py-Nd thin films have good soft magnetic properties when the Nd dopants increase up to 11.6%. The room-temperature saturation magnetization M_s decreases significantly from around 7.26×10^5 A/m to 3.80×10^5 A/m when the Nd content increases to 11.6%. The local anisotropy of Nd atomic impurities leads to a dispersion of Py magnetic moments [19]. This sperimagnetism [23] order leads to a decreasing saturation magnetization with increasing Nd content. The details of the analysis of the magnetization are presented elsewhere.

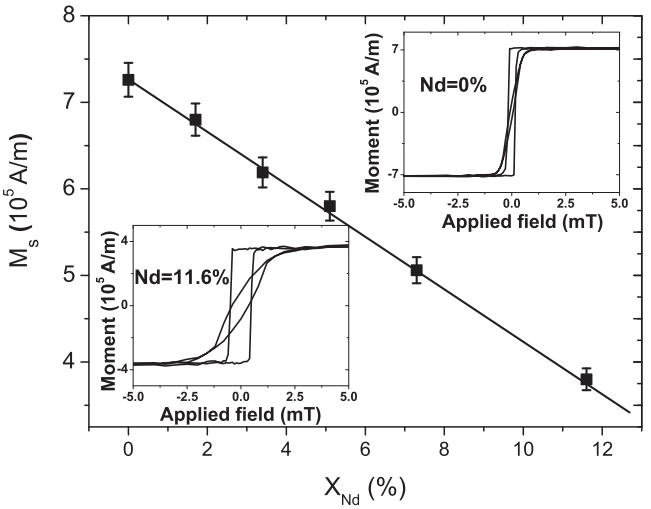

FIG. 2. Saturation magnetization M_s for Nd_x-$Py_{(1-x)}$ thin films. The inset is the in-plane hysteresis loops along the easy-axis and hard-axis directions. The coercive field increases from the polycrystalline phase of pure Py ($H_c = 0.17$ mT) to $H_c = 0.48$ mT in the amorphous phase with $X_{Nd} = 11.6\%$.

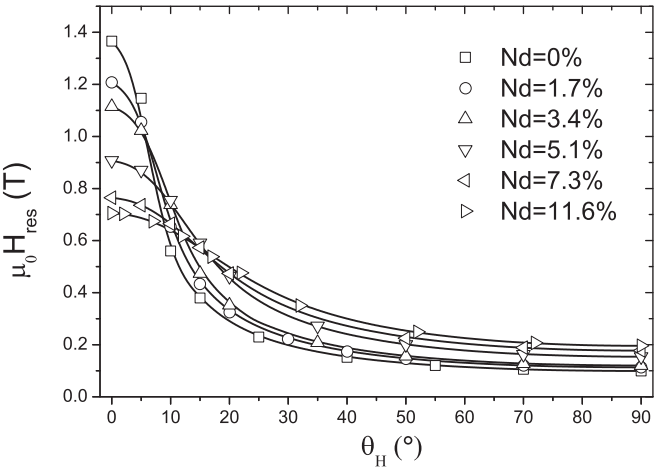

FIG. 3. Angular dependence of the resonance field on out-of-plane orientation θ_H with increasing Nd content. Here, $\theta_H = 0^\circ$ represents the direction of the film normal, $\theta_H = 90^\circ$ represents the direction of the film plane. The symbols are experimental data and the solid lines are theoretical fitting curves according to Eq. (3).

B. Angular dependence of ferromagnetic resonance spectra

FMR measurements for all films were performed at 9.78 GHz for various field orientations, including in-plane and out-of-plane orientations, at room temperature. Figure 3 exhibits the dependence of FMR resonance field $\mu_0 H_{\rm res}$ on out-of-film-plane field orientation θ_H. The dots refer to the experimental data and the lines are the theoretical fitting curves utilizing Eq. (3). It is found that the resonant field in the film normal decreases as Nd content increases, while in parallel geometry $\mu_0 H_{\rm res}$ increases slightly, which is mainly caused by the decrease of the effective magnetization which is shown in Table I.

The motion of the magnetization around its equilibrium position is described by the Landau-Lifshitz-Gilbert (LLG) equation of motion:

$$\frac{d\vec{M}}{dt} = -\gamma \vec{M} \times \vec{H}_{\rm eff} + \frac{\alpha}{M_s}\left(\vec{M} \times \frac{d\vec{M}}{dt}\right). \qquad (1)$$

The first term is the torque referring to the precession of the magnetization in the effective field $\vec{H}_{\rm eff}$, and the second term is its dissipation torque. The constant γ is the gyromagnetic ratio, α is the Gilbert damping parameter, and M_s is the saturation magnetization.

The free energy density of our system for fitting the experimental data includes the following terms:

$$F = -\vec{M} \cdot \vec{H} + 2\pi M_s^2 \cos^2\theta + (K_1 \sin^2\theta + K_2 \sin^4\theta). \qquad (2)$$

Here, θ is the angle of the magnetization vectors in spherical coordinates with respect to the film normal. The first term is the Zeeman energy, the second term is the demagnetizing energy, and the terms in parentheses are the first- and second-order magnetic anisotropy energy including the volume magnetocrystalline anisotropy and the surface anisotropy. The out-of-plane resonance field $H_{\rm res}$ is obtained by solving the LLG equation and minimizing the total free energy density F [24]:

$$\left(\frac{\omega}{\gamma}\right)^2 = [H\cos(\theta - \theta_H) - 4\pi M_{\rm eff}\cos 2\theta + H_{k2}(3\sin^2\theta\cos^2\theta - \sin^4\theta)][H\cos(\theta - \theta_H) - 4\pi M_{\rm eff}\cos^2\theta + H_{k2}\sin^2\theta\cos^2\theta], \qquad (3)$$

where $4\pi M_{\rm eff} = 4\pi M_s - 2K_1/M_s$, $H_{k2} = 4K_2/M_s$, and θ_H is the angle of the applied field.

By fitting our experimental data with Eq. (3), we obtained the effective magnetization $4\pi M_{\rm eff}$, the first- and second-order magnetic anisotropy constants K_1 and K_2, as well as the Lande g factor as shown in Table I.

From Table I, we see that as the Nd content increases from 0% to 11.6%, the magnetic anisotropy constants K_1 and K_2 change from negative to positive, which means the easy axis of the magnetic anisotropy changes from the easy film plane ($K_1 < 0$, $K_2 < 0$) to the easy film normal ($K_1 > 0$, $K_2 > 0$) when the Nd content increases to 5.1%. However, the demagnetizing field in the normal direction, $4\pi M_s$, is larger than the magnetic anisotropy field and thus the preferred direction of the magnetization vector is always in plane for all films. The Lande g factor increases slightly from 2.11 to 2.16 when the Nd content increases to 11.6%, which implies that the effective orbital moment increases with increasing Nd content.

The FMR linewidth (Fig. 4) exhibits an angular dependence with a clear maximum at 10° to 30° with respect to the film normal. The linewidth and the peak width of the curve increase as the Nd content increases. It is well known that the relaxation mechanisms of the magnetization are reflected in the FMR linewidth, which include intrinsic Gilbert-type and extrinsic non-Gilbert-type mechanisms. In general, three contributions

TABLE I. Parameters obtained from theoretical fitting.

Nd concentration	0%	1.7%	3.4%	5.1%	7.3%	11.6%
$4\pi M_s$ (10^6 A/m)	9.12	8.55	7.78	7.29	6.36	4.78
$4\pi M_{\rm eff}$ (10^6 A/m)	9.78	8.77	7.84	6.82	5.78	3.84
K_1 (10^3 J/m^3)	−23.73	−7.54	−1.93	13.72	14.77	17.86
K_2 (10^3 J/m^3)	−3.74	3.23	−1.04	2.73	3.01	4.82
g	2.11	2.11	2.11	2.12	2.12	2.16
$\Delta\theta_H$ (10^{-3} rad)	0.0	2.0	1.4	1.8	3.4	5.5
$\Delta 4\pi M_{\rm eff}$ (10^4 A/m)	0.30	0.28	1.31	2.16	1.74	3.87
Damping α (10^{-3})	7.0	26.4	73.3	110.1	130.8	177.6

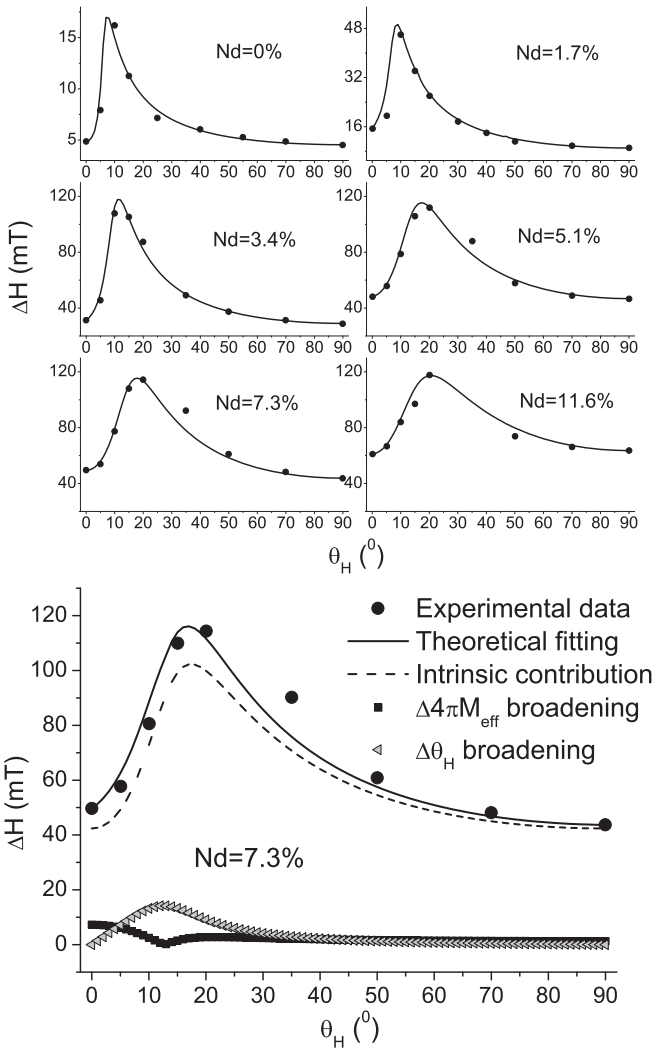

FIG. 4. (a) Angular dependence of linewidth ΔH on out-of-plane orientation θ_H with increasing Nd content. (b) Angular dependence of the intrinsic linewidth and inhomogeneous linewidth broadening at $X_{Nd} = 7.3\%$.

are considered:

$$\Delta H = \Delta H_{\text{Gilb}} + \Delta H_{2\text{mag}} + \Delta H_{\text{inhom}}. \quad (4)$$

The first term is the intrinsic linewidth due to Gilbert damping related to spin-orbit coupling, which transfers the energy of the precessing magnetization to the lattice and refers to the dissipation of magnetic energy. The second term is an extrinsic contribution due to two-magnon scattering, and the last term is the inhomogeneous linewidth broadening resulting from the inhomogeneity of the films.

The two-magnon scattering is a process where a uniform magnon (wave vector $k = 0$) excited by FMR scatters into $k \neq 0$ magnons, resulting in an additional contribution to the FMR linewidth $\Delta H_{2\text{mag}}$ [25]. For the FMR linewidth with main contributions from two-magnon scattering, there is a larger broadening in the parallel configuration of the film and no contribution to the perpendicular configuration, $\Delta H_{2mag\perp} = 0$; thus, $\Delta H_\perp < \Delta H_\parallel$ [26]. For our films we find that $\Delta H_\perp$ is slightly bigger than $\Delta H_\parallel$, which indicates that the contribution of two-magnon scattering could be neglected.

The inhomogeneous linewidth broadening ΔH_{inhom} can be expressed as follows [24]:

$$\Delta H_{\text{inhom}} = \left|\frac{\partial H}{\partial \theta_H}\right| \Delta\theta_H + \left|\frac{\partial H}{\partial 4\pi M_{\text{eff}}}\right| \Delta 4\pi M_{\text{eff}}, \quad (5)$$

where $\Delta\theta_H$ represents the spread in the orientations of the crystallographic axes among various grains, and $\Delta 4\pi M_{\text{eff}}$ represents the inhomogeneity of the local demagnetizing field. For inhomogeneous films one expects a larger inhomogeneous broadening near the perpendicular configuration compared to the parallel configuration, which shows that $\Delta H_\perp > \Delta H_\parallel$ [24,27,28]. For our films it shows that $\Delta H_\perp$ is slightly bigger than $\Delta H_\parallel$, which indicates that the inhomogeneous linewidth broadening does exist but is small. This can be understood, since our films are either polycrystalline or amorphous.

As shown in Fig. 4(a), the fitting curves (solid lines) agree with the experimental data well, and the intrinsic contribution ΔH_{Gilb} is separated from expression (4) by neglecting $\Delta H_{2\text{mag}}$. It is shown more clearly in Fig. 4(b), where the angular-dependent intrinsic linewidth ΔH_{Gilb} and inhomogeneous linewidth including $\Delta\theta_H$ broadening and $\Delta 4\pi M_{\text{eff}}$ broadening are drawn separately from the theoretical fitting. The parameters $\Delta\theta_H$ and $\Delta 4\pi M_{\text{eff}}$ related to the inhomogeneous linewidth broadening increase with increasing Nd concentration, which indicates that the homogeneity of the film becomes worse with increasing Nd concentration. This might be because the Nd dopants change the film crystalline structure from polycrystalline to amorphous and make the film become more inhomogeneous. Although the $\Delta\theta_H$ and $\Delta 4\pi M_{\text{eff}}$ show an increasing trend, the whole contribution of the inhomogeneous linewidth broadening is very small compared to the intrinsic linewidth, which indicates that the intrinsic contribution ΔH_{Gilb} plays the main role in the measured linewidth. The Gilbert damping factor α, calculated from ΔH_{Gilb}, increases from 0.0070 to 0.1776 (about 25-fold enhanced), as shown in Fig. 5 and Table I.

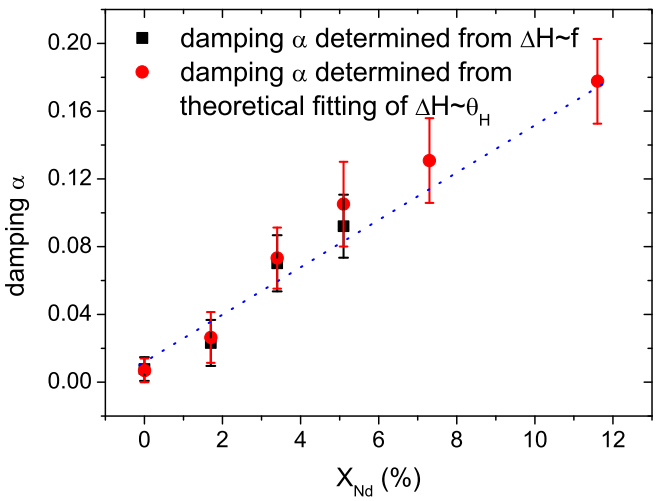

FIG. 5. (Color online) Damping parameter α for Nd_x-$Py_{(1-x)}$ thin films. The error bar is about 10% by calculation of α from the fitting of linewidth.

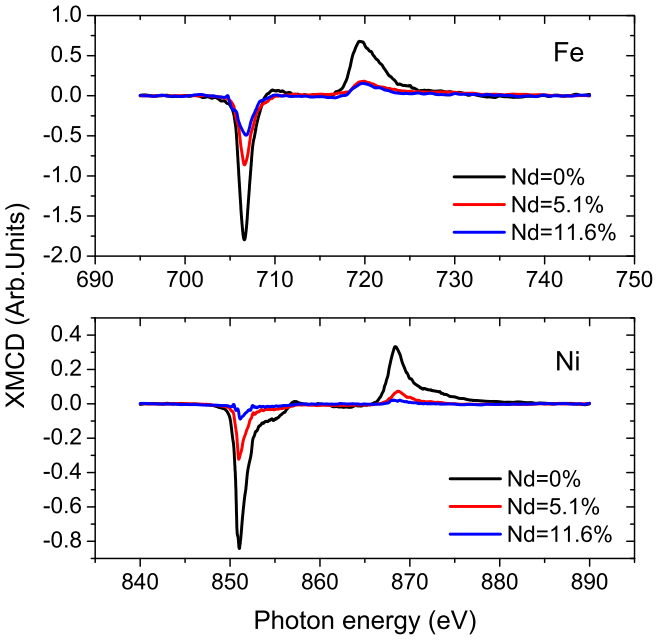

FIG. 6. (Color online) XMCD spectra at the Fe and Ni $L_{2,3}$ edges for Nd_x-$Py_{(1-x)}$ thin films at room temperature; the Nd concentrations are 0%, 5.1%, and 11.6%, respectively.

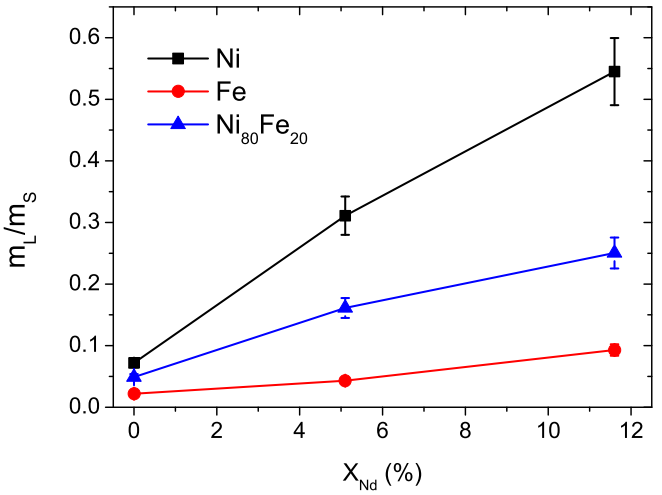

FIG. 7. (Color online) The orbital-to-spin moment ratio at room temperature; the Nd concentrations are 0%, 5.1%, and 11.6%, respectively. The black squares represent the m_L/m_S of Ni, the red dots refer to the m_L/m_S of Fe, and the blue triangles represent the m_L/m_S of $Ni_{80}Fe_{20}$. The error bar for m_L/m_S is estimated to be around 10%, taking into account the inaccuracies in the sum rules analysis, the error in the calculated number of empty 3*d* states, etc.

The contribution to the damping parameter per concentration of Nd dopant can be described as $\alpha = \alpha_{Py} + \Delta\alpha_{Nd}X_{Nd}$. From Woltersdorf's work, the $\Delta\alpha$ for Gd, Tb, Dy, and Ho doping are 0.0005, 0.038, 0.036, and 0.017, respectively[10]. For our samples the value of $\Delta\alpha_{Nd}$ is 0.015, which indicates that the contribution for Nd dopant is similar to that for Ho and larger than that for Gd but smaller than that for Tb and Dy. One of the most interesting points is that Nd and Ho possess the same total orbital moment $L = 6$; it seems that the orbit-orbit coupling between the conduction electrons and the impurity ions [9] is the main mechanism leading to the damping enhancement. However, Tb with a twofold smaller total orbital moment $L = 3$ has a threefold stronger effect on the damping in Py thin films, which means the RE dopants with larger L do not always make the damping of Py-RE film have larger enhancement, which is not consistent with the orbit-orbit mechanism [9]. We speculate that the spin-orbit coupling may be one of the main mechanisms responsible for our giant enhancement of the intrinsic damping parameter in Py films doped by Nd, which seems to be confirmed by our results on x-ray magnetic circular dichroism (XMCD) measurements as shown in Fig. 6.

Due to its unique ability to separate the orbital and spin moments for each element in a multielement compound [29], XMCD is an ideal tool to study the changes in the spin-orbital coupling in our Nd_x-$Py_{(1-x)}$ thin films. The measurements were taken at remanence in the total-electron-yield mode at beam line I1011 of the MAX Laboratory in Lund, Sweden. The angle of incidence of the x-ray beam was set to 60° relative to the sample surface normal. XMCD is the difference in the absorption of the left and right circularly polarized x rays. The spectra taken at the Fe and Ni $L_{2,3}$ absorption edges for Nd_x-$Ni_{80}Fe_{20(1-x)}$ thin films are displayed in Fig. 6. Using the sum rules analysis on these spectra [30,31], we have obtained the orbital and spin moments of Fe and Ni, respectively, and the resulting orbital-to-spin moment ratio is shown in Fig. 7. We found that the orbital-to-spin moment ratio (m_L/m_S) of Fe and Ni in Nd-doped Py films increases significantly with the increasing Nd concentration, indicating that the spin-orbit coupling is enhanced by Nd dopants. Moreover, we find that the m_L/m_S of $Ni_{80}Fe_{20}$ is fivefold enhanced with 11.6% of Nd, while the Gilbert damping factor α obtained from FMR is about 25-fold enhanced, which is consistent with the spin-orbit mechanism; the Gilbert damping factor α is proportional to $(m_L/m_S)^2$ [32,33]. Our results indicate that the damping enhancement in Nd-doped Py is mainly due to the spin-orbit coupling. However, the damping in RE-doped TM films is very complex and is not controlled by a single mechanism. Other mechanisms such as the "slow relaxing impurity model" [10] may provide partial contributions, and need further research later.

C. Frequency dependence of ferromagnetic resonance and two-magnon scattering

The intrinsic damping parameter of the magnetization can be better probed with the frequency-dependent FMR linewidth measurements, because the Gilbert contribution ΔH_{Gilb} is linearly proportional to the microwave frequency. Contributions due to defects and magnetic inhomogeneity are believed to be independent of frequency and are often expressed as a constant linewidth term $\Delta H(0)$ [34]. The simple relationship can be expressed as follows [35–37]:

$$\Delta H = \Delta H(0) + \alpha\frac{\omega}{\gamma}, \tag{6}$$

where the linear term is assumed to be a measure of the intrinsic damping and the magnitude of $\Delta H(0)$ depends on the film quality and approaches zero for the perfect samples.

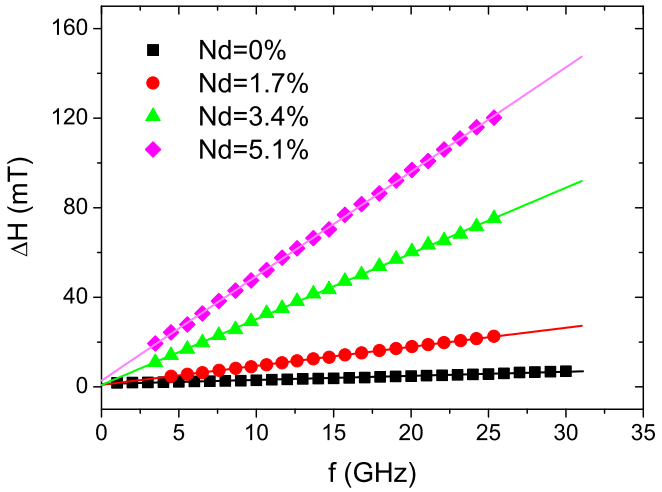

FIG. 8. (Color online) FMR linewidth ΔH with the frequency f up to 26 GHz.

Figure 8 shows the FMR linewidth as a function of frequency for Nd-doped Py films with various Nd concentrations in our experiment. The linewidth strongly increases with increasing Nd concentration and, with the given doping level, it linearly depends on the frequency up to 26 GHz. For all films the linewidth extrapolated to zero frequency $\Delta H(0)$ is very small and can be neglected. The damping parameter α is determined from the slope of the frequency-dependent linewidth, which agrees well with our fitted results from field-orientation-dependent FMR linewidth with fixed frequency, as shown in Fig. 5.

In order to further study the contributions of two-magnon scattering on the FMR linewidth, we calculate the behavior of the FMR linewidth described by two-magnon scattering. The frequency dependence of the two-magnon process is not linear in ω. It shows a nonlinear slope at low frequencies and saturation at high frequencies, which can be described by the following expression [38]:

$$\Delta H_{2\mathrm{mag}}(\omega) = \Gamma \sin^{-1}\sqrt{\frac{[\omega^2+(\omega_0/2)^2]^{1/2}-\omega_0/2}{[\omega^2+(\omega_0/2)^2]^{1/2}+\omega_0/2}}, \qquad (7)$$

where $\omega_0 = \gamma 4\pi M_{\mathrm{eff}} = \gamma(4\pi M_s - 2K_1/M_s)$. If $\omega \ll \omega_0$, then expression (7) shows that the linewidth should vary linearly with frequency, similar to the prediction of the LLG equation. However, if $\omega \sim \omega_0$, it exhibits substantial deviations from linear behavior in this regime. The effective magnetization $4\pi M_{\mathrm{eff}}$ can be determined by analyzing the angular-dependent FMR resonance field as shown in Table I. The factor Γ is the strength of the two-magnon scattering along the in-plane crystallographic direction, which is fitted to the experimental data. In order to find out whether the $\Delta H_{2\mathrm{mag}}$ contributions exist, first we could assume the contributions did exist, then calculate the value of ω_0 and compare with the frequency dependence of the linewidth data for the $\omega \sim \omega_0$ range. By substituting those parameters obtained from experimental data, we get the value of ω_0; thus, the value of $f_0 = \omega_0/2\pi$ is obtained and its value decreases from 28.8 to 11.7 GHz as the Nd content increases from 0% to 11.6%. However, as shown in Fig. 8, the frequency dependence of the FMR linewidth ΔH shows a linear behavior of $\Delta H \sim f$ instead of the curves with substantial deviations, which indicates that the two-magnon scattering contribution is very small and can be neglected.

IV. CONCLUSION

In summary, we have studied in detail the effects of permalloy thin films by light rare-earth Nd doping in the dilute region. As Nd content increases, the structure of the films changes from polycrystalline to amorphous rapidly and the magnetization M_s reduces linearly, while high hysteresis squareness along the in-plane easy axis and low H_c are kept. The first- and second-order magnetic anisotropy constants K_1 and K_2 increase from negative to positive, which implies that the perpendicular anisotropy is enhanced due to the Nd dopants. The doping-level-dependent Lande g factor indicates that the effective orbital moment increases with increasing Nd content. Three different mechanisms of ferromagnetic resonance linewidth have been discussed. The values of the Gilbert damping parameter α, obtained by theoretical fitting of angular-dependent FMR linewidth and variable-frequency FMR measurements, are very similar and can be enhanced remarkable by Nd doping. Our results show that low Nd doping in permalloy can enhance the Gilbert damping while keeping the soft magnetic properties of permalloy films.

ACKNOWLEDGMENTS

We thank F. Römer and R. Salikhov for helpful comments. This work is supported by NBRP (Grant No. 2010CB923404) and NSFC (Grants No. 50871029 and No. 51322206), NSFC Grant for Young Scientists (Grant No. 61306121) and China Postdoctoral Science Foundation (Grant No. 2013M541580).

[1] C. Back, R. Allenspach, W. Weber, S. Parkin, D. Weller, E. Garwin, and H. Siegmann, Science **285**, 864 (1999).
[2] R. H. Koch, G. Grinstein, G. A. Keefe, Y. Lu, P. L. Trouilloud, W. J. Gallagher, and S. S. P. Parkin, Phys. Rev. Lett. **84**, 5419 (2000).
[3] G. E. Rowlands and I. N. Krivorotov, Phys. Rev. B **86**, 094425 (2012).
[4] S. Chikazumi, *Physics of Ferromagnetism*, 2nd ed. (Oxford University Press, Oxford, 2009), p. 565.
[5] A. Lyberatos, J. Magn. Magn. Mater. **246**, 303 (2002).
[6] Q. Peng and H. N. Bertram, J. Appl. Phys. **81**, 4384 (1997).
[7] W. Bailey, P. Kabos, F. Mancoff, and S. Russek, IEEE Trans. Magn. **37**, 1749 (2001).
[8] S. E. Russek, P. Kabos, R. D. McMichael, C. G. Lee, W. E. Bailey, R. Ewasko, and S. C. Sanders, J. Appl. Phys. **91**, 8659 (2002).
[9] A. Rebei and J. Hohlfeld, Phys. Rev. Lett. **97**, 117601 (2006).

[10] G. Woltersdorf, M. Kiessling, G. Meyer, J.-U. Thiele, and C. H. Back, Phys. Rev. Lett. **102**, 257602 (2009).
[11] I. Radu, G. Woltersdorf, M. Kiessling, A. Melnikov, U. Bovensiepen, J.-U. Thiele, and C. H. Back, Phys. Rev. Lett. **102**, 117201 (2009).
[12] M. O. A. Ellis, T. A. Ostler, and R. W. Chantrell, Phys. Rev. B **86**, 174418 (2012).
[13] S. G. Reidy, L. Cheng, and W. E. Bailey, Appl. Phys. Lett. **82**, 1254 (2003).
[14] J. Russat, G. Suran, H. Ouahmane, M. Rivoire, and J. Sztern, J. Appl. Phys. **73**, 1386 (1993).
[15] Y. Fu, L. Sun, J. Wang, X. Bai, Z. Kou, Y. Zhai, J. Du, J. Wu, Y. Xu, H. Lu, and H. Zhai, IEEE Trans. Magn. **45**, 4004 (2009).
[16] C. Luo, D. Zhang, Y. Wang, H. Huang, Y. Zhai, and H. Zhai, J. Alloys Compd. **598**, 57 (2014).
[17] I. Campbell, J. Phys. F **2**, L47 (1972).
[18] H.-S. Li, Y. Li, and J. Coey, J. Phys.: Condens. Matter **3**, 7277 (1991).
[19] R. C. Taylor, T. R. McGuire, J. M. D. Coey, and A. Gangulee, J. Appl. Phys. **49**, 2885 (1978).
[20] J. Lindner, R. Meckenstock, and M. Farle, in *Characterization of Materials*, edited by E. N. Kaufmann (Wiley, New York, 2013), pp. 1–20.
[21] M. Farle, T. Silva, and G. Woltersdorf, in *Magnetic Nanostructures* (Springer, New York, 2013), pp. 37–83.
[22] Z. Feng, J. Hu, L. Sun, B. You, D. Wu, J. Du, W. Zhang, A. Hu, Y. Yang, D. Tang *et al.*, Phys. Rev. B **85**, 214423 (2012).
[23] J. Coey, J. Appl. Phys. **49**, 1646 (1978).
[24] C. Chappert, K. L. Dang, P. Beauvillain, H. Hurdequint, and D. Renard, Phys. Rev. B **34**, 3192 (1986).
[25] M. Sparks, *Ferromagnetic Relaxation Theory* (McGraw-Hill, New York, 1966).
[26] P. Landeros, R. E. Arias, and D. L. Mills, Phys. Rev. B **77**, 214405 (2008).
[27] J.-M. Beaujour, D. Ravelosona, I. Tudosa, E. E. Fullerton, and A. D. Kent, Phys. Rev. B **80**, 180415 (2009).
[28] K. Ounadjela, Y. Henry, M. Farle, and P. Vennegues, J. Appl. Phys. **75**, 5601 (1994).
[29] W. Zhang, S. A. Morton, P. J. Wong, B. Lu, Y. Xu, M. P. de Jong, W. G. van der Wiel, and G. van der Laan, J. Phys. D **46**, 405001 (2013).
[30] B. T. Thole, P. Carra, F. Sette, and G. van der Laan, Phys. Rev. Lett. **68**, 1943 (1992).
[31] P. Carra, B. T. Thole, M. Altarelli, and X. Wang, Phys. Rev. Lett. **70**, 694 (1993).
[32] C. Kittel, Phys. Rev. **76**, 743 (1949).
[33] M. Farle, Rep. Prog. Phys. **61**, 755 (1998).
[34] B. Heinrich, J. F. Cochran, and R. Hasegawa, J. Appl. Phys. **57**, 3690 (1985).
[35] R. D. McMichael, D. J. Twisselmann, and A. Kunz, Phys. Rev. Lett. **90**, 227601 (2003).
[36] W. Platow, A. N. Anisimov, G. L. Dunifer, M. Farle, and K. Baberschke, Phys. Rev. B **58**, 5611 (1998).
[37] R. Urban, B. Heinrich, G. Woltersdorf, K. Ajdari, K. Myrtle, J. F. Cochran, and E. Rozenberg, Phys. Rev. B **65**, 020402 (2001).
[38] R. Arias and D. L. Mills, Phys. Rev. B **60**, 7395 (1999).